Food Chemistry: X 22 (2024) 101380

Contents lists available at ScienceDirect

Food Chemistry: X

journal homepage: www.sciencedirect.com/journal/food-chemistry-x

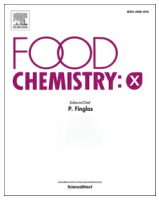

Removal of Cu (II) by ion exchange resin and its re-utilization of the residual solution from the distilled *Lycium barbarum* wine

Yan Dang [a], Qing-An Zhang [a,*], Zhi-Hui Zhao [b]

[a] *Institute of Food & Physical Field Processing, School of Food Engineering and Nutrition Sciences, Shaanxi Normal University, Xi'an 710062, Shaanxi Province, PR China*

[b] *Ningxiahong Medlar Industry Group Company Limited, Zhongwei 755100, Ningxia Province, PR China*

ARTICLE INFO

Keywords:
Distilled residual
Ceramic membrane filtration
Resin adsorption
Recombined brandy
Physicochemical properties
Re-utilization

ABSTRACT

In order to re-utilize the residual from the distillation of the Chinese wolfberry wine and reduce the environmental pollution, the residual is firstly filtered by the ceramic membrane of 50 nm, then the Cu (II) has transferred from the distillation is removed using the ion exchange resin, and the treated solution is recombined with the distilled liquor to make the Chinese wolfberry brandy and the comparison has conducted on the physicochemical properties, antioxidant activity and flavor compounds between the recombined brandy and the finished brandy. The results indicate that the Cu (II) was effectively removed by ceramic membrane combined with the D401 resin. Compared with finished brandy, the recombined brandy contains high contents of polysaccharides, phenols and flavonoids, thus contributing to the improvement of antioxidant capacity. The gas chromatography-ion mobility spectrometry (GC-IMS) reveals that 25 volatile compounds like esters and alcohols have identified in the brandy samples, and the differences are significant between the recombined and the finished brandy. In summary, the distilled residual from the Chinese wolfberry wine might be re-used after the appropriate treatment so as to reduce the discharge and environmental pollution.

1. Introduction

Chinese wolfberry, a treasured botanical originating from China, has been extensively utilized as a traditional Chinese medicine herbal and a functional food, revered for its diverse benefits including antioxidation properties and anti-aging effects. (Niu, Huang, Jin, Wu, & Zhou, 2017). Brandy, renowned for its distinctive flavor profile, is a spirit crafted through the fermentation and distillation of grapes, standing proudly among the world's six most celebrated distilled spirits (Dziekonska-Kubczak, Pielech-Przybylska, Patelski, & Balcerek, 2020). Typically, the name of the brandy is paired with its primary ingredient, such as jujube brandy or plum brandy; hence, Chinese wolfberry brandy is a unique liquor distilled from fresh wolfberry fruit (Vyviurska, Matura, Furdíková, & Špánik, 2017; Xia, Suo, Wang, Cerbin, & Wang, 2017). Owing to the transfer of bioactive components from the raw materials into the wine during fermentation, Chinese wolfberry brandy boasts exceptional characteristics that distinguish it from other spirits (Zhao et al., 2019).

Distilled residual, which contains valuable nutrient compounds such as polysaccharides, phenols and flavonoids has been generated during the brewing process, but the natural discharge of these residual will not only pollute the environment but also cause a large loss of resources (Salian, Wani, Reddy, & Patil, 2018). The flavonoids and related phenolic and polyphenolic compounds have been of interest owing to their antimicrobial, antioxidative, anti-inflammatory, and anti-mutagenic properties, there is an extensive literature describing each of these biological properties (Lorenzo, Colombo, Biella, Stockley, & Restani, 2021; Lee et al., 2017; Rodriguez-Mateos et al., 2014). And numerous researches have indicated that dietary polyphenols or metabolites and catabolites of flavonoids achieve health promotion through gut microbiota regulation, for example, dietary flavonoids are enzymatically hydrolyzed and absorbed in the intestine, and are conjugated to their glucuronide/sulfate forms by phase II enzymes in epithelial cells and the liver (Li et al., 2023; Murota, Nakamura, & Uehara, 2018).

In addition, the presence of copperware distillation equipment in winemaking can result in elevated levels of Cu (II) in wine. The appropriate amount of Cu (II) catalyzes the color, taste, and flavor of the final distilled wine product, enhancing their quality and sensory characteristics (Neves, Oliveira, Fernandes, & Nóbrega, 2007; Szymczycha-

* Corresponding author.
E-mail address: qinganzhang@snnu.edu.cn (Q.-A. Zhang).

https://doi.org/10.1016/j.fochx.2024.101380
Received 1 March 2024; Received in revised form 9 April 2024; Accepted 9 April 2024
Available online 12 April 2024

Madeja, Welna, Jamroz, Lesniewicz, & Pohl, 2015). However, excessive concentrations of Cu (II) adversely affect its stability, organoleptic properties, and poses risks to the human digestive, nervous, and immune system (Bonic et al., 2013; Wang et al., 2023; Wang et al., 2023). ICP-OES testing has revealed that the distillation residual contains Cu (II) at a concentration of 154.58 mg/mL. However, there is little research has been done on removing metal ions from brandy distillation residuals. It is important to carefully consider the selection of treatment methods and optimize the process to minimize costs and environmental impact while protecting the safety and quality of the final product.

Membrane technology is widely used in the food industry for juice clarification and concentration processes due to its advantages of preserving the product's quality, decreasing equipment costs, and improving aroma retention (Bhattacharjee, Saxena, & Dutta, 2017a; Bhattacharjee, Saxena, & Dutta, 2017b). For example, membrane separation has been applied to concentrate pomegranate and watermelon juice while maintaining their bioactive compounds content (Bhattacharjee et al., 2017a; Bhattacharjee et al., 2017b; Cassano, Conidi, & Tasselli, 2014). Resin adsorption, utilizing ion exchange and microporous resins, is an effective and eco-friendly technology widely employed in the food industry, specifically in alcoholic beverages, to reduce acidity and improve flavor (Zhong, Li, Yang, & Li, 2018). Additionally, resin adsorption has been showed to reduce metals content in wine (Benitez, Castro, & Barroso, 2001; Palacios, Caro, & Perez, 2000). Further research is necessary to determine the optimal condition and parameters for combining membrane separation and resin adsorption, as there is limited literature regarding the approach for wastewater treatment in food industry. The development of new alcoholic beverages can be facilitated by the utilization of treated solution, such as the production of de-protein whey beverage from dairy whey wastewater treated by UF (Korotkov, Stanislavskaya, & Melnikova, 2015). The sensory properties and antioxidant capacity of the recombined brandy can be enhanced by incorporating volatile flavor compounds and nutrients derived from treated solution. Based on the above facts, it can be deduced that the Cu (II) in the wastewater could be removed and the nutrient composition preserved through the implementation of an appropriate technique. As a result, the comprehensive utilization rate and added value of wastewater can be improved.

Gas chromatography-ion mobility spectrometry (GC-IMS) is an emerging technology that has been developed for the accurate separation of volatile compounds from complex samples and to analyze them (Guo, Schwab, Ho, Song, & Wan, 2022). It offers the advantage of low detection limits and high separation performance of GC and high sensitivity of IMS. In recent years, broader applications of GC-IMS have been observed in various fields such as medicine, cosmetics and environmental protection, with a particular focus on food flavor analysis (Wang, Chen, & Sun, 2020). For example, the correlation between characteristic volatile compounds and brandy aging has been identified using GC-IMS (Chen et al., 2021; Chen et al., 2021; Li, Yang, Tian, Zou, & Li, 2020). Previous studies have demonstrated that GC-IMS exhibits higher reliability in studying volatile flavor, and it represents a promising approach for the identification of brandy quality.

The main objective of this research is to utilize membrane technology for the filtration of distillation residual, as well as the removal of Cu (II) and retention of nutrients from treatment water using ion exchange resin. Subsequently, a Chinese wolfberry brandy will be developed with the treatment water as the major components. Additionally, the nutritional components and antioxidant activity of recombined and finished Chinese wolfberry brandy were compared and analyzed, and a comprehensive understanding of the diversity of flavor compounds was sought using GC-IMS. The innovation of this paper lies in the combination of ceramic membrane filtration and ion exchange resin adsorption, which can not only reduce the loss of nutrients, but also effectively remove Cu (II) in distillation residue, meeting the national food safety standards and enabling the recycling of distillation residue from brandy production. These efforts will contribute to recycle nutrients in distillation residual, reduce wastewater discharge, decrease environmental pollution, and enhance the added value of wolfberry.

2. Experiments

2.1. Chemicals and materials

The distilled residual, distilled liquor (the original brandy with high alcohol content after secondary distillation) and finished brandy were supported by Ningxiahong Medlar Industry Group Company Ltd. (Ningxia, China). The ion exchange resins, glucose, rutin, gallic acid and 1,1-diphenyl-2-picrylhydrazyl were purchased from Yuanye Bio-Technology Co. Ltd. (Shanghai, China). Folin-Ciocalteu reagent was obtained from Biotopped Technology Co. Ltd. (Beijing, China). Sodium hydroxide, hydrochloric acid, phosphoric acid (H_3PO_4) and sodium carbonate (Na_2CO_3) were purchased from Tianli Chemical Reagent Co. Ltd. (Tianjin, China). All other chemicals and solvents were of analytical grade.

2.2. Ceramic membrane treatment of distillation residual

A ceramic membrane with a pore size of 50 nm and a pressure of 0.5 MPa was utilized to separate the distillation residual, and the ceramic membrane filtrate (CMF) and ceramic membrane concentrate (CMC) were collected and stored at 4 °C for further use. The characteristics of the CMC and CMF had been reported in our paper (Dang, Zhao, Dong, Dang, & Zhang, 2022). The levels of Cu (II) in the CMC and CMF were determined by ICP-OES to be 117.67 mg/mL and 62.25 mg/mL, respectively. In the following experiment, CMF was taken as the research object to further explore the adsorption process of ion exchange resin for Cu (II) in CMF.

2.3. Static adsorption and desorption tests

The static adsorption and desorption capacity of 4 different resins for Cu (II) were evaluated. Specifically, 0.3 g of pre-treated resin was added into a 25 mL CMF solution, and the suspension was subjected to adsorption for 6 h in a constant temperature oscillator. The residual concentration of metal ions in the solution was detected using Inductively Coupled Plasma-Optical Emission Spectrometer (ICP- OES). Experiments were performed in triplicate for the sake of accuracy. Once equilibrium was achieved, the resins were rinsed with deionized water and subsequently eluted with a 10% HCl solution. The concentration of Cu (II) in the eluent was determined, and several parameters were calculated, including adsorption capacity, adsorption ratio and desorption ratio.

$$Q = (C_0 - C_e)\cdot V_a / W \tag{1}$$

$$A = (C_0 - C_e)/C_0 \times 100\% \tag{2}$$

$$D\% = C_d V_d / [(C_0 - C_e)\cdot C_0] \times 100\% \tag{3}$$

The following parameters were determined: where Q、A、and D represent the adsorption capacity (Q) in mg/g, adsorption ratio (A) in % and desorption ratio (D) in %. The variables used in the calculations were as follows: C_0, the initial concentration of Cu (II) before adsorption in mg/g, C_e, the concentration of Cu (II) at adsorption equilibrium in mg/g, C_d, the concentration of Cu (II) in eluent in mg/g; V_a, the volume in mL of CMF solution, V_d, the volume in mL of desorption solution; and W, the weight in g of resin.

2.4. Batch adsorption experiments

Batch adsorption experiments were conducted in triplicate using CMF solution to investigate the adsorption behavior of the Cu (II) by D401 resin. The effect of adsorption dose (0.1–0.5 g), pH (3–9), contact

time (0–480 min) and adsorption temperature (15, 25 and 35 °C) on the adsorption behavior of Cu (II) were examined to determine the optimal adsorption conditions. Additionally, the adsorption kinetics curve of Cu (II) on D401 was studied by shaking 0.3 g of D401 resin with 25 mL of CMF solution at 293 K, and the samples were taken at different intervals until adsorption equilibrium was reached (Hoang, Nishihama, & Yoshizuka, 2021). The pseudo-first order and pseudo-second-order model was represented by eq. (4) and (5).

$$ln(Q_e - Q_t) = lnQ_1 - k_1 t \tag{4}$$

$$t/Q_t = 1/(k_2 Q_2^2) + t/Q_2 \tag{5}$$

where Q_e and Q_t represent the amounts of Cu (II) ions adsorbed on the resin at equilibrium and at various times t (mg/g), respectively. Q_1 and Q_2 are the calculated adsorption capacity of the pseudo-first-order model and the pseudo-second-order model (mg/g), respectively; while k_1 and k_2 are the rate constants of the pseudo-first-order model (1/min) and the pseudo-second-order model (mg/ (g min)). The fitting validity of these models is commonly assessed by the plotting of $ln(Q_e - Q_t)$ vs t and t/Q_t vs t, respectively.

For the adsorption isotherms, 25 mL of CMF solution with varying concentrations (39.62, 62.52, 78.94, 101.2 and 117.6 mg/mL) was added to a conical flask containing D401 resin. These concentrations were determined based on preliminary experiments conducted in our laboratory. The Langmuir and Freundlich models can be expressed as follows (Wang, Jia, et al., 2023; Wang, Ma, et al., 2023):

$$C_e/Q_e = 1/(K_L Q_m) + C_e Q_m \tag{6}$$

$$lnQ_e = lnk_f + 1/(nlnC_e) \tag{7}$$

where Q_e is the equilibrium adsorption capacity (mg/g), C_e is the equilibrium concentration (mg/g), K_L is the Langmuir constant, K_f is the Freundlich constant and n is the characteristic constant.

The adsorption thermodynamics were investigated by studying the adsorption of Cu (II) onto D401 resin at various temperatures (15, 25 and 35 °C). Eqs. (8)、(9) were used to calculate the thermodynamic parameters for the adsorption of Cu (II) onto the D401 resin, including ΔG (kJ·mol^{-1}), ΔS (J·mol^{-1}·K^{-1}) and ΔH (kJ·mol^{-1}), were calculated with the following equations(He et al., 2014):

$$\Delta G = -RTlnK_L \tag{8}$$

$$lnK_L = \Delta S/R - \Delta H/(R \cdot T) \tag{9}$$

where R (8.314 J/mol · K) is the gas constant, T (K) stands for the absolute temperature, and K_L (L/mg) is the standard thermodynamic equilibrium constant defined by Q_e / C_e The values ΔH and ΔS can be calculated from the slope and intercept of Vant's Hoff plots of ln K_L vs T / 1.

2.5. Preparation of recombined brandy

To obtain the recombined brandy, the raw materials were blended according to the eq. (10). Among them, M and A represent the quality and alcohol content of the recombined brandy respectively, M_1 and A_1 represent the quality and alcohol content of the original brandy (OB), and M_2 and A_2 represent the quality and alcohol content of the treatment liquid.

$$\begin{cases} M_1 \times A_1\% + M_2 \times A_2\% = M \times A\% \\ M_1 + M_2 = M \end{cases} \tag{10}$$

2.6. Determination of physicochemical parameters

The pH value was measured using a PHS-3C digital pH meter (Shanghai Leici Co. Ltd., China); titratable acidity (TA) was determined through titration with 0.01 M NaOH and expressed as a percentage of acetic acid (Fan, Zhang, Yan, & Tian, 2016); total soluble solids (TSS) was measured using a digital refractometer(Shanghai Leici Co. Ltd., China); the content of reducing sugar was determined using the dinitro salicylic (DNS) method (Chen et al., 2018); the alcoholic content was tested using an alcohol meter, and the results were expressed as milliliters of alcohol per 100 mL of wine; the CIE parameters (L*, a* and b*) were determined by a SC-80C automatic colorimeter (Beijing Kangguang instrument Co. Ltd., China).

2.7. Determination of the active ingredient

The total polyphenolic content (TPC) of samples was determined using the Folin-Ciocalteu method with some minor modifications (Fan et al., 2016); the total flavonoid content (TFC) was determined using $AlCl_3$ colorimetric method with slight modifications (Kwaw et al., 2018); the total polysaccharides content (TSC) was measured by a phenol-sulfuric acid method, with several modifications (Zhang, Zhang, Yan, & Fan, 2017).

2.8. Determination of antioxidant activities

2.8.1. Ferric-reducing antioxidant power

The ferric-reducing antioxidant power (FRAP) was determined with slight modifications (Chen, Huang, Yang, & Hou, 2019). Samples with volumes of 0.1, 0.2, 0.3, 0.4, 0.5 and 0.6 mL were supplemented with distilled water to 1 mL. 2.5 mL phosphate buffer (0.2 mol/L, pH = 6.6) and 2.5 mL potassium ferrocyanide (1%, *w/v*) were added, respectively. After 20 min of incubation at 50 °C, 2.5 mL trichloroacetic acid (10%, *w/v*) was added, and the reaction solution was centrifuged at 3000 r/min for 10 min. Then, 2.5 mL supernatant was collected and mixed with 2.5 mL distilled water and 0.5 mL ferric chloride solution (0.1%, w/v). Finally, the absorbance at 700 nm was recorded after 10 min of reaction. 0.1 mg/mL GA was used as a positive control.

2.8.2. DPPH radical scavenging assay

The DPPH free radical-scavenging activity of the samples was measured according to the method (Yang, Su, Wang, Wang, & Wang, 2021), with slight modifications. Samples with volumes of 0.1, 0.2, 0.3, 0.4, 0.5, and 0.6 mL were supplemented with distilled water to 1 mL and mixed with 4 mL DPPH (10^{-4} M) respectively. Then, the mixture was remined in the dark for 30 min. 0.1 mg/mL GA was used as a positive control. The absorbance was determined at 517 nm. The DPPH scavenging rate of the sample can be calculated by the following formula:

$$\text{Scavenging rate } (\%) = 1 - (A_s - A_b)/A_0 \tag{11}$$

A_s: Absorption of sample solution.
A_b: Absorption of DPPH replaced by ethanol.
A_0: Absorption of sample replaced by ethanol.

2.8.3. Hydroxyl radical scavenging

Hydroxyl radical scavenging activity was determined using the method with slight modifications (Zhang, Fan, Zhao, Wang, & Liu, 2013). Samples with volumes of 0.1, 0.2, 0.3, 0.4, 0.5 and 0.6 mL were added distilled water to 1 mL. Then 1 mL of $FeSO_4$(9^{-3} M), 1 mL of H_2O_2(1%, w/v) and 1 mL of salicylic acid (70% ethanol solution) were added to the mixture and reacted for 25 min at 37 °C. The absorbance was measured at 510 nm. 0.1 mg/mL GA was used as a positive control. The scavenging rate was calculated by the following formula:

$$\text{Scavenging rate } (\%) = 1 - (A_s - A_b)/A_0 \tag{12}$$

A_s: Absorption of sample solution.
A_b: Absorption of H_2O_2 replaced by distilled water.
A_0: Absorption of sample replaced by distilled water.

2.8.4. Superoxide anion scavenging assay

The scavenging activity was measured as the method described in the paper (Yang et al., 2021), with some modifications. Samples with volumes of 0.1, 0.2, 0.3, 0.4, 0.5 and 0.6 mL and supplemented with distilled water to 1 mL. Then 4 mL of Tris-HCl buffer (0.05 M, pH 8.2) and 3 mL of pyrogallol solution (30 mM) were added to the sample. After a 5-min reaction, 0.5 mL of HCl was added to the mixture to terminate the reaction. The absorbance was determined at 320 nm. 0.1 mg/mL GA was used as a positive control. The scavenging rate was calculated by the following formula:

$$\text{Scavenging rate } (\%) = 1 - (A_s - A_b)/A_0 \quad (13)$$

A_s: Absorption of sample solution.

A_0: Absorption of sample replaced by ethanol.

2.9. Determination of volatile profiles

The volatile profiles of brandy were analyzed using a GC-IMS system (FlavourSpec®, G.A.S, Dortmund, Germany) equipped with an autosampler (CTC Analytics AG, Zwingen, Switzerland) and a WAX capillary column (30 m × 0.53 mm, 1 μm, Restek, Beijing, China)0.100 μL brandy sample was added to a 20-mL headspace injection vials. After incubating at 60 °C and 500 rpm for 15 min, a 100 μL headspace was injected by a syringe previously heated to 85 °C. Then the headspace was delivered to the GC for pre-separation. The column was maintained at 45 °C and the carrier gas (N_2, 99.99% pure) flow ramp was optimized as follows: 2 mL/min in the first 2 min, 10 mL/min within 2–10 min, and finally increased to 100 mL/min within 20 min. The ionization source operated in positive ion mode using a β-ray (3H, 300 MBq). The drift tube temperature and drift gas (N_2) flow rate were set 45 °C and 150 mL/min, respectively.

To calculate the retention indices (RIs) of volatile compounds in brandy samples, an external standard of n-ketone (C_4-C_9, Sinopharm Group Co. Ltd., Beijing, China) was used in the Laboratory Analysis View software (FlavourSpec®, Dortmund, Germany). The type of each volatile compound was confirmed by comparing the RIs and drift time of the authentic standard compounds with the GC-IMS library G.A.S (Dortmund, Germany). Qualitative analysis was conducted based on the NIST database and IMS database of the GC-IMS Library Search application software. The extraction and analysis of the GC-IMS data were performed using the LAV software (version 2.2.1, G.A.S, Dortmund, Germany) to generate a topographic plot and gallery plot, providing corresponding information for the VOCs. The composition of volatile substances in the brandy sample was determined and analyzed, and the relative content of each volatile component was calculated by peak volume normalization.

2.10. Calculation of relative odor activity value (ROAV)

The VOCs' $ROAV_{max}$ that contributed the most to the flavor of the sample was defined as 100, and the ROAV of other VOCs was calculated as follow (Song et al., 2022):

$$ROAV \approx 100 \times \frac{C_i}{C_{max}} \cdot \frac{T_{max}}{T_i} \quad (14)$$

In the formula, C_i is the relative content of the aroma compound in tea (%); T_i is the aroma threshold of compound in water (mg/kg); C_{max} and T_{max} represent the relative content and aroma threshold of the compound that contributes the most to the overall flavor of the sample.

2.11. Data analysis

Statistical significance between groups was performed by one-way ANOVA, and $P < 0.05$ was considered statistically significant. Analysis of variance (ANOVA) was conducted using the SPSS statistics software of version 11.0 (SPSS Inc., Chicago, IL, USA).

3. Results and discussion

3.1. Adsorption and desorption capacities of different resins

The corresponding model and parameter performance of the four resins are shown in Table 1. Resin adsorption had widely utilized in the wastewater industry due to its numerous advantages, including high adsorption efficiency, simplicity, speed, versatility, and chemical stability, and had become a research hotspot for the removal of heavy metals in wastewater treatment (Bao et al., 2020; Chu, Feng, Liu, Wu, & Liu, 2022). The adsorption effects of the four resins on Cu (II) and the retention of active components are shown in Fig. 1. As shown in Fig. 1 (a), it is obvious that the adsorption capacities and de-adsorption capacities of the D401 resins were higher than those of the 001 × 7、732 and D101 resins, reaching 97% adsorption rate and 81% desorption rate. As depicted in Fig. 1(b), the loss of phenolic compounds had minimal for all four resins, while the loss of flavonoid compounds was more significant. This was due to the van der Waals force and hydrogen bonding interaction between resins and phenolic compounds, and it had commonly used in the enrichment and purification of plant active ingredients (Luo et al., 2019). Therefore, the retention effect of active components was optimal with the D401 resin. However, Cu (II) existed in distillation residues with complex matrix compounds. It was well-known that the matrix effect not only significantly affects the targeted removal of specific components in such mixtures, but may also cause false quantified results (Mao et al., 2021; Schimek et al., 2016). For instance, polyphenols contain dense ortho-hydroxyphenyl and meta-hydroxyphenyl groups, which can act as multi-base ligands and form cyclic chelates with metal ions (Chen, Farag, et al., 2021; Chen, Li, et al., 2021; Zhang, Guan, Jiang, & Khan, 2023). Therefore, it was a good research direction to study the impact of matrix compound removal on the assay results in subsequent experiments.

3.2. Adsorption performance

To investigate the impact of adsorbent dose on the efficiency of adsorption process, the adsorbent dose was varied from 100 mg to 500 mg while keeping all other parameters constant. The results for adsorption capacities and removal efficiencies of Cu (II) at the equilibrium were presented in Fig. 2(a), as the removal efficiency of Cu (II) increased from 88.52% to 97.41%, while the equilibrium adsorption concentration decreased from 7.15 to 1.61 mg/L. This could be attributed to the fact that increasing the adsorbent dose provides a large surface area and more binding sites for Cu (II) in solution (Bansal, Singh, & Garg, 2009). However, it was important to note that the Environmental Protection Agency and World Health Organization have defined the maximum allowable level of Cu (II) in natural water as 1.0–2.0 mg/L (Katiyar et al., 2021). Therefore, for the treatment of Cu (II) in wastewater, an optimal condition of approximately 0.3 g of resin was chosen.

The initial solution pH was an important parameter that had been reported to influence the adsorption of metal ions (El-Ashtoukhy, Amin, & Abdelwahab, 2008). In this study, we investigated the adsorption of

Table 1
Physical properties of the four kinds of resins.

Resin	Surface area (m^2/g)	Particle diameter(mm)	Polarity	Appearance
001 × 7	10–100	0.45–1.25	Polar	Golden yellow globular particles
732	5–30	0.3–1.2	Polar	Light yellow globular particles
D101	100–1500	0.30–1.25	Non-polar	White opaque globular particles
D401	30–120	0.03–0.12	Non-polar	Light yellow opaque globular particles

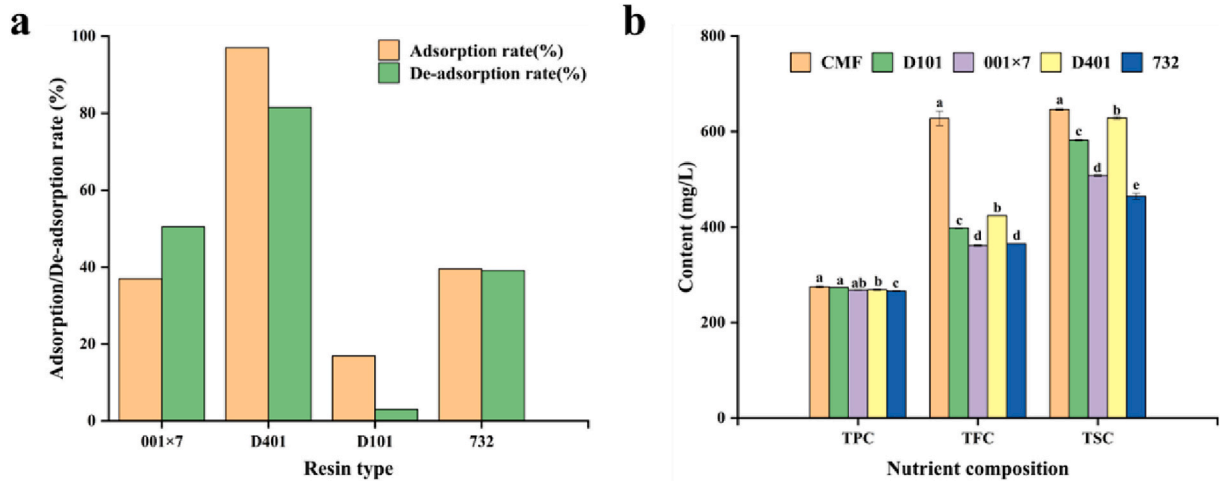

Fig. 1. Effects of different resin on the filtrate (a) Absorption and desorption capabilities; (b) Nutrient composition.

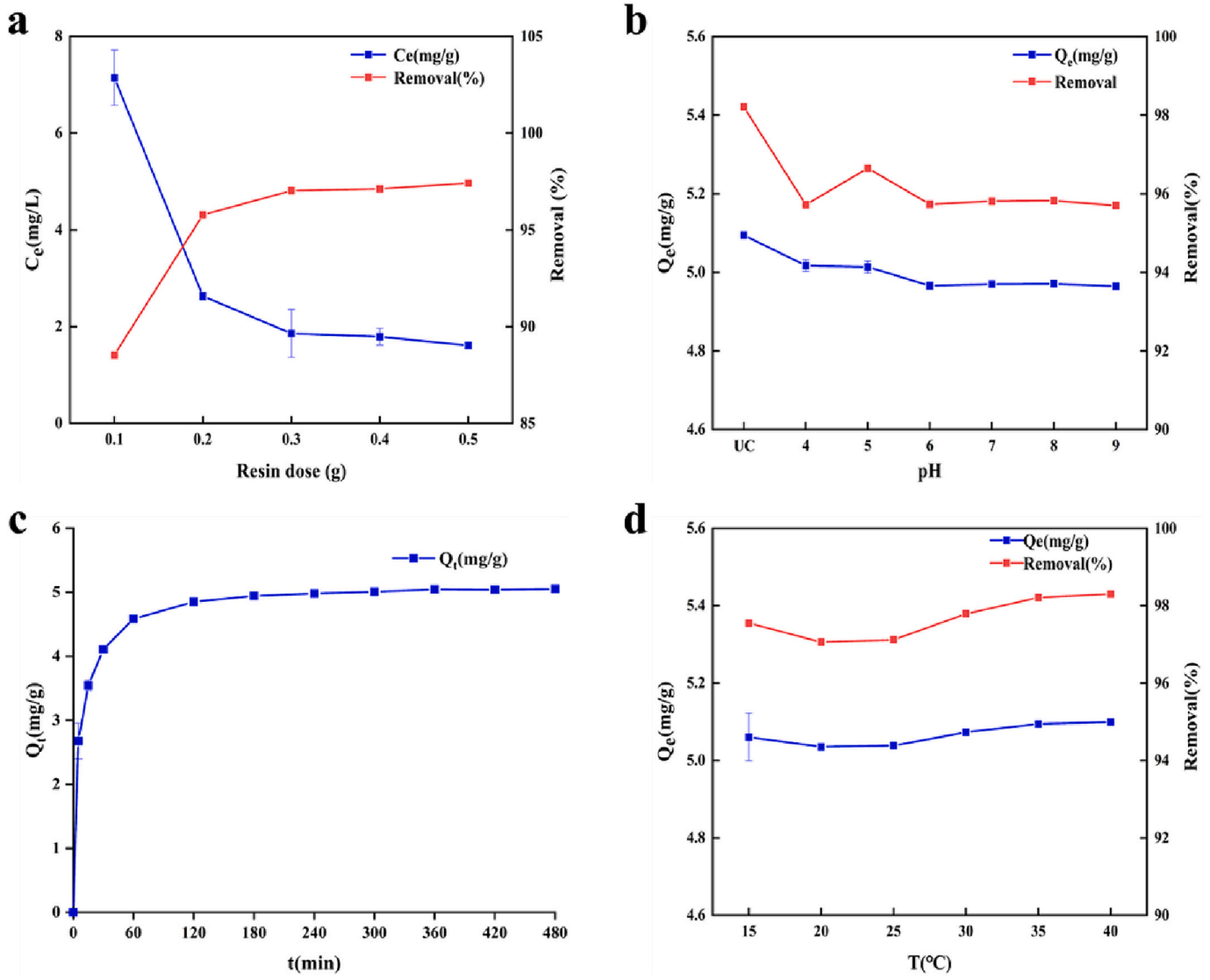

Fig. 2. Effect of (a) resin dose, (b) pH, (c) contact time, (d) temperature on the adsorption of Cu (II) (conditions: C_0:62.52 mg·L^{-1}; resin dosage:0.3 g; pH:3.4; T:25 °C).

Cu (II) over the range of initial solution pH 2–9. Fig. 2(b) shows that the adsorption capacity of resin for Cu (II) gradually decreased with the maximum adsorption capacity observed at pH without adjusting. At lower pH levels, both carboxylic groups and nitrogen atoms were protonated, resulting in less availability of active sites for metal ions due to greater repulsive forces (He et al., 2014). Conversely, when the pH value exceeded the threshold for metal precipitation, the removal process could be considered a combination of adsorption and precipitation of metal hydroxides, making accurate measurement impossible (Liang, Song, Huang, Li, & Chen, 2013).

Fig. 2(c) presents the results of investigating the removal of Cu (II) by D401 resin as a function of contact time. Contact time was varied in the range of 5–480 min. The adsorption amount of resin gradually increased with increasing contact time, and saturation adsorption was ultimately reached after 180 min. The initial period of 0–60 min had identified as the rapid adsorption stage, during which the adsorption amount increased rapidly with increasing contact time. As the reaction time continued to increase, the number of available active sites on the adsorbent gradually decreased until they were completely exhausted (Wang, Jia, et al., 2023; Wang, Ma, et al., 2023).

The effect of contact temperature on the Cu (II) adsorption process was investigated in the temperature range of 15–40 °C. As depicted in Fig.2(d), the adsorption capacity of Cu (II) increased at temperature of 20–40 °C. This can be attributed to the greater swelling of resin at higher temperatures, which enhances the diffusion of Cu (II) into the resin (He et al., 2014). Consequently, the finding indicated that the adsorption of Cu (II) onto D401 was more effective at higher temperatures.

3.3. Adsorption kinetics

The parameters of kinetic models and their corresponding R^2 values obtained from the related plots are given in Table 2, and the simulated plots for the pseudo-first-order and pseudo-second-order models are displayed in S.1(a) and S.1(b). The results suggested that the kinetic data of Cu (II) adsorption were better fitted by the pseudo-second-order model (R^2 = 0.9999) compared to the pseudo-first-order (R^2 = 0.9445). Additionally, the calculated maximum adsorption amount (Qe^{cal}) closely matched the experimentally determined values (Q_e^{exp}). The finding suggested that chemisorption was the dominant rate-controlling step in the uptake of Cu (II) by D401 resin (An et al., 2020).

3.4. Adsorption isotherms

The adsorption isotherm represented the relationship between the equilibrium adsorption capacity and the equilibrium concentration at a constant temperature. The calculated parameters for both Langmuir and Freundlich isotherms models were summarized in Table 3, and the fitting of the Langmuir and Freundlich isotherms data were displayed in S.2(a) and S.2(b). The results revealed that the adsorption capacities of Cu (II) onto resin increased with increasing initial concentrations of Cu (II). Furthermore, the Langmuir model better represented the adsorption of Cu (II) by resin, as it provided much higher correlation coefficients (R^2 = 0.9593–0.9989). These findings indicated that the adsorption occurred at the homogeneous surface of D401 resin, and the Cu (II) was adsorbed in a monolayer form on the resin (An et al., 2020).

Table 3
Isotherm constants evaluated for Cu (II) adsorption on D401 resin.

T (°C)	Langmuir			Freundlich		
	q_m (mg/g)	R_L	R^2	K_F	n	R^2
15	7.72	0.4615	0.9989	2.3610	2.3507	0.8679
25	9.34	0.4167	0.9980	2.5886	1.9320	0.9268
35	10.13	0.6255	0.9593	3.4795	1.8149	0.9410

3.5. Adsorption thermodynamics

The calculated values of thermodynamic parameters had presented in Table 4. The ΔG values at different temperatures were negative, indicating a spontaneous adsorption process. As the temperature increased, the absolute value of ΔG gradually increased, indicating that higher temperature was more favorable to the adsorption reaction. The positive values of ΔH revealed that the adsorption was an endothermic process. Moreover, the positive values of ΔS demonstrated that the adsorbent had good affinity for Cu (II).

3.6. Physicochemical characteristics of different brandy

The physicochemical parameters of original brandy (OB), finished brandy (FB), ceramic membrane concentrate brandy (CMCB) and ceramic membrane filtrate brandy (CMFB) were shown in Table 5. The values of L*, a* and b*in OB and CMCB showed no significant differences, and were higher than CMFB. Compared to the OB, the CMCB and CMFB had higher phytochemical concentrations, the reason is that phenolic compounds were transferred from Chinese wolfberry to brandy during the maceration, but a high proportion of these compounds remained in the byproducts (Jara-Palacios, 2019). However, the content of total sugars and polysaccharides in FB is higher than in CMCB and CMFB, the reason is that FB had added sugar in the post-processing.

3.7. Antioxidant activities of different brandy

It's well known that brandy contains a number of key functional components, mainly including polysaccharides, phenolics and flavonoids. These components can not only control the stability of the wine, and improve the organoleptic properties, but also have a major effect on the antioxidant properties of brandy (Niu et al., 2017). Fig. 3 shows the antioxidant capacities of different brandy. Generally, FRAP was regarded as a significant indicator of potential antioxidant activity (Hifney, Fawzy, Abdel-Gawad, & Gomaa, 2016). As shown in Fig. 3(a), FRAP increased with increasing sample volume in an obvious dose-dependent manner. At a given concentration, the samples demonstrated FRAP in the following order: CMFB>CMCB>GA > FB. Compared to the positive control of GA, the FRAPs of CMFB and CMCB were slightly higher at lower volume, whereas the FRAP of GA exceeded both at higher volume.

Table 4
Adsorption thermodynamic parameters of Cu (II) adsorbed onto D401 resin.

T (°C)	T (K)	lnK_L	ΔG(kJ/mol)	ΔH (kJ/mol)	ΔS [J/(mol·K)]
15	288	1.77	−4.25		
25	298	2.32	−5.58	74.12	270.65
35	308	3.79	−9.72		

Table 2
Kinetic parameters for the adsorption of Cu (II) (conditions: C_0:51.60 mg·L^{-1}; resin dosage:0.3 g; pH:3.4; T:25 °C).

Kinetic model	Q_e^{exp} (mg/g)	Pseudo-first-order kinetics			Pseudo-second-order kinetics		
Adsorbate		Q_e^{cal} (mg/g)	k_1 (min^{-1})	R^2	Q_e^{cal} (mg/g)	k_2 (g/mg·min)	R^2
Cu (II)	5.053	1.4450	0.0127	0.9445	5.1203	0.0302	0.9999

Table 5
Physicochemical parameters of different brandy.

Brandy	OB	CMCB	CMFB	FB
pH	4.00 ± 0.01^{c}	4.38 ± 0.01^{a}	4.37 ± 0.01^{a}	4.18 ± 0.00^{b}
TSS (%)	20.33 ± 0.14^{a}	14.98 ± 0.02^{c}	14.67 ± 0.36^{c}	17.17 ± 0.14^{b}
Alcohol(% vol)	65.23 ± 0.15^{a}	31.13 ± 0.05^{c}	31.27 ± 0.23^{c}	35.63 ± 0.15^{b}
CIE				
L*	91.29 ± 0.12^{c}	92.40 ± 0.01^{ab}	92.62 ± 0.36^{a}	91.91 ± 0.58^{bc}
a*	6.92 ± 0.05^{ab}	6.57 ± 0.39^{b}	4.41 ± 0.51^{c}	7.70 ± 0.98^{a}
b*	13.63 ± 1.30^{a}	5.74 ± 0.54^{bc}	6.90 ± 0.61^{b}	4.48 ± 1.12^{c}
TS (g/L)	0.24 ± 0.00^{d}	2.01 ± 0.01^{b}	1.58 ± 0.01^{c}	3.46 ± 0.01^{a}
TA (g/L)	0.29 ± 0.00^{d}	3.29 ± 0.06^{a}	3.01 ± 0.09^{b}	0.41 ± 0.00^{c}
TPC (mg/L)	18.56 ± 1.43^{d}	265.44 ± 16.55^{a}	254.53 ± 14.92^{b}	120.65 ± 2.26^{c}
TFC (mg/L)	16.32 ± 0.71^{d}	448.97 ± 7.23^{a}	353.41 ± 12.96^{b}	56.89 ± 2.22^{c}
TSC (mg/L)	46.56 ± 5.49^{d}	408.92 ± 5.82^{b}	293.87 ± 8.87^{c}	506.34 ± 21.95^{a}

a-d different letters next to mean values indicates statistically significant difference ($p < 0.05$).

Fig. 3(b) indicated the scavenging effect on •DPPH. Overall, the capacities of DPPH free radical scavenging increased with the increase of brandy volume. The capacities of free radical scavenging of FB were 6–14%, and CMCB and CMFB were 11.7–46.4% and 11.4–43.7%, while GA had the highest scavenging ability up to 24.9–90%. Therefore, the mixed brand had higher antioxidant activity, related to the high content of phenolics and flavonoids in the distillate waste. As shown in Fig. 3(c), all of the samples generally were found to have a certain capacity to scavenge the hydroxyl radical. The scavenging effect of GA was the best. The antioxidant activity of FB and GA increased slowly, while the two mixed brandies increased sharply with the increase of brandy volume. When the additive amount was <0.4 mL, the antioxidant capacity of FB was higher than mixed brandy, whereas the latter outweighed the former when the sample volume was >0.4 mL. It can be seen that the scavenging rate of three brandies to superoxide anion has not high within the experimental concentration range, the maximum was not >30%. The scavenging capacity was as follows: CMFB>CMCB>FB, and the scavenging effect of GA was the best. The antioxidant activity of three brandies increased slowly with the increase of brandy volume. The scavenging effect of the sample on superoxide anion may be attributed to the active hydroxyl groups in the phenolic and flavonoid compounds (Fan et al., 2016).

3.8. *Differential analysis of topographic plots of volatile components in brandy*

The volatile flavor of different brandies was analyzed using the GC-IMS method in order to identify difference in flavor substances. The

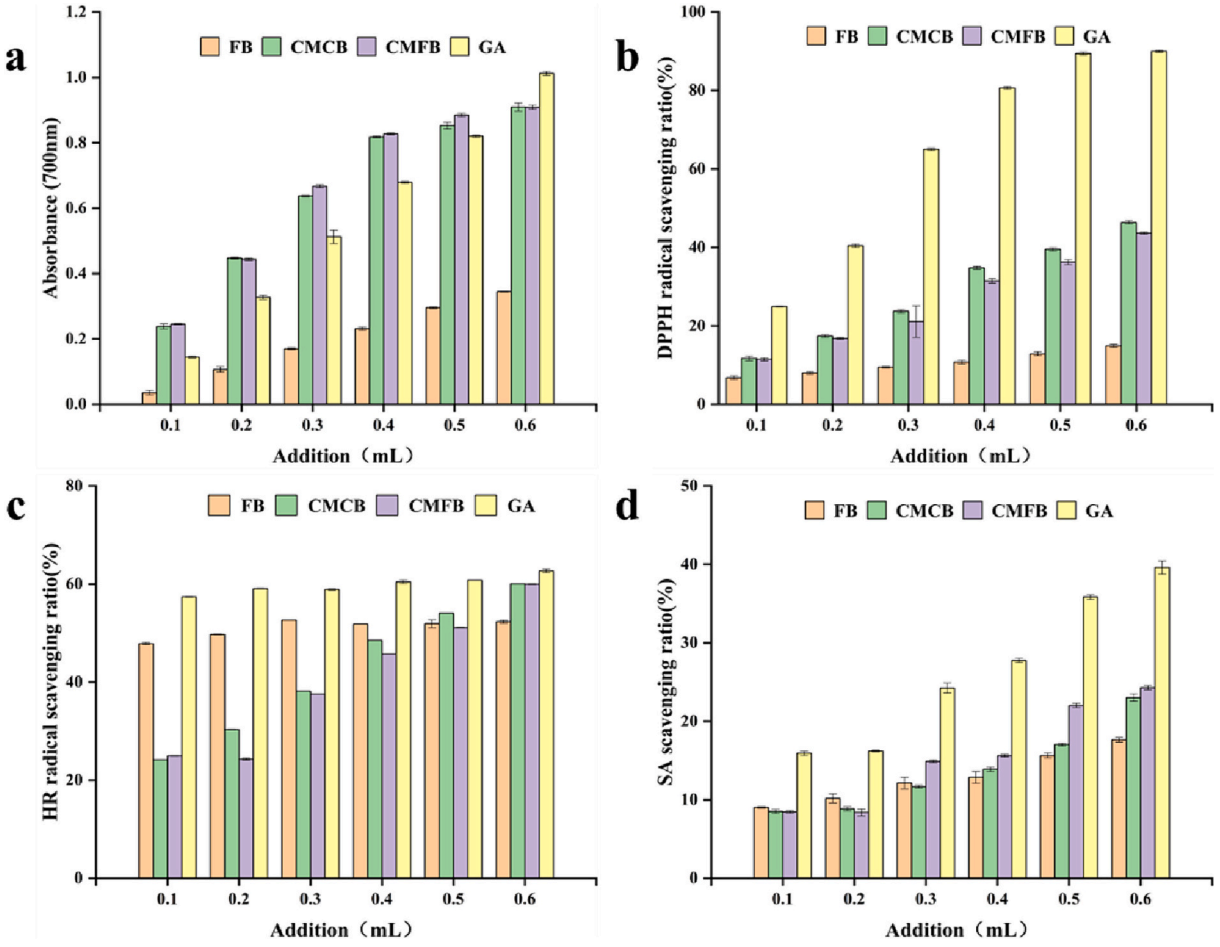

Fig. 3. Antioxidant capacities of different brandy(a) ferric-Reducing Antioxidant Power; (b) DPPH radical scavenging capacity; (c) hydroxyl radical scavenging ability; (d) superoxide anion scavenging ability.

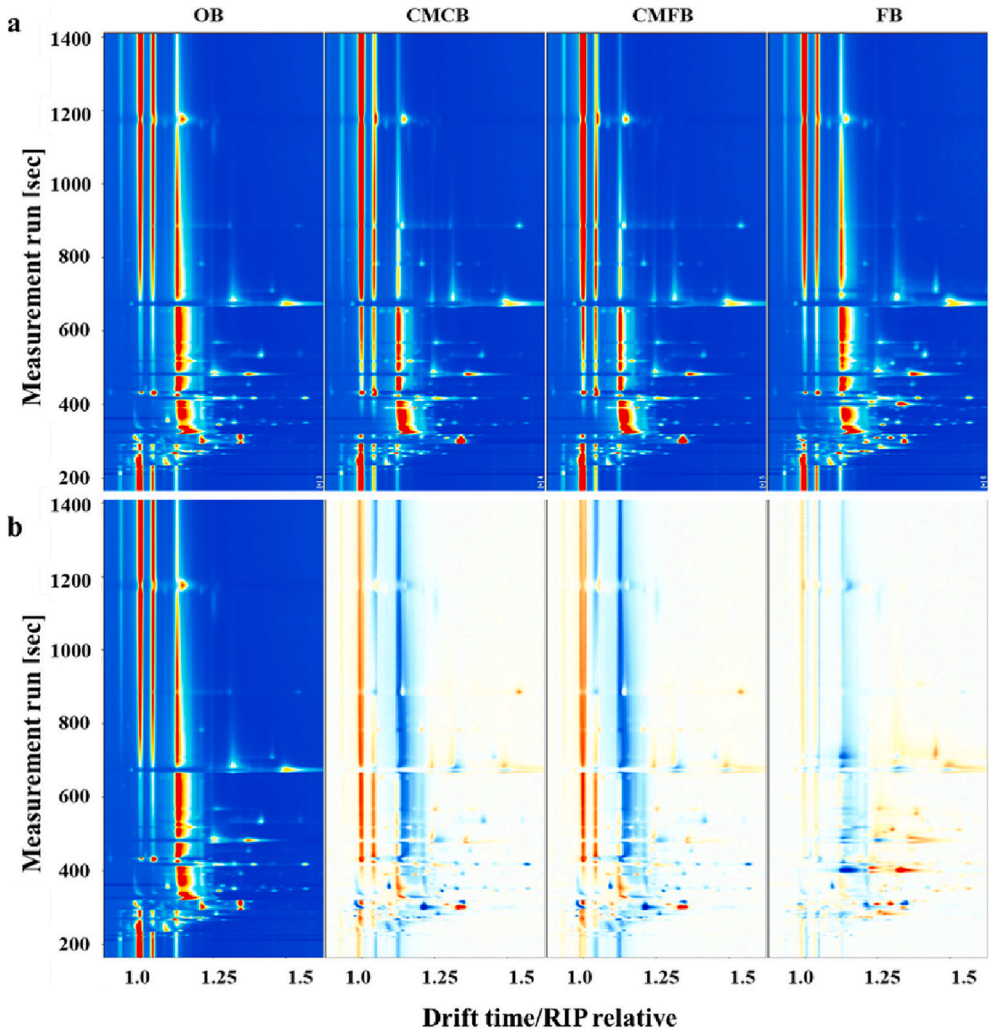

Fig. 4. Volatile compounds in brandy (a)topographic plots of GC-IMS; (b) comparison results under the spectral diagram.

results obtained from the GC-IMS analysis are presented in Fig. 4, which shows a topographic plot. In the plot, the horizontal coordinate represented the ion migration time, while the vertical coordinate represented the gas chromatography retention time. Fig. 4(a) had indicated that the majority of signals appeared in the retention time of 200–600 s and the drift time of 1.0–1.5. The color represented the concentration of the substance, with darker color indicated higher concentration. The concentration was positively correlated with the concentration of volatile organic compounds detected in the sample, providing insights into the flavor profiles of the brandies (Chen, Farag, et al., 2021; Chen, Li, et al., 2021).

The difference comparison model was employed to assess the flavor ingredients of samples. The topographic plot of OB served as a reference, against which the topographic plot of other samples was compared. In the resulting plot Fig. 4(b), red indicated a higher concentration of the substance compared to the reference, which blue signified a lower concentration. The analysis revealed that the flavor of the four samples exhibited similarities but differed in terms of odor strength. Specifically, CMCB and CMFB contained a higher number of volatile components compared to FB. Furthermore, for CMCB and CMFB, most of the peaks were similar but different in concentration.

3.9. Analysis of differences in the composition of volatile compounds of different brandies

The aromatic compounds in brandy basically consist of fruit-derived volatiles and the volatiles produced during the fermentation and distillation (Ren et al., 2018). The chemical characteristics of the bandy were presented in Table 6, and the mean values and standard deviations calculated for each volatile compound of brandy were shown. As seen in Fig.5 (a), a total of 25 volatile were detected by qualitative analysis, including 7 esters, 7 alcohols, 5 aldehydes, 3 ketones, 2 acids, and 1 sulfur-containing compound. Esters and alcohols were the most abundant groups in brandy, followed by aldehydes, ketones and acids, it was consistent with previous research (Raičević, Popović, Jančić, Šuković, & Pajović-Šćepanović, 2022). The FB showed a significantly higher content of volatile esters and alcohols compared with the other samples. The total peak area of aroma rank: FB>CMCB>CMFB>OB(Fig.5 (b)).

Esters: Esters were mainly produced by both fermentation and distillation and had typical odors such as fruit and floral descriptors (Matijasevic et al., 2019). In this study, a total of seven ester compounds were detected in brandy, and the total concentration of the volatile esters in the CMCB, CMFB and FB was clearly greater than in the OB. The Ethyl acetate, Ethyl butyrate, Ethyl caproate, Ethyl isobutyrate, Ethyl lactate, and Ethyl propionate were identified as the important esters in brandy and play a key role in the organoleptic characteristics of newly distilled brandy (Zhao, Zheng, Song, Sun, & Tian, 2018). The presence of Ethyl acetate made a significant contribution to the volatile profile of distilled alcoholic beverages. The relative content of Ethyl acetate quantified in CMCB and CMFB (16%) exceeded by over 2 times that detected in the FB (6.9%), whereas the relative content of ethyl caproate in FB (6.3%) was >15 times that of CMCB and CMFB (0.4%). The reason

Table 6
Analysis of volatile components of four brandies by GC-IMS.

No	Compounds	Threshold	CAS	Formula	RT [s]	DT [ms]	OB		CMCB		CMFB		FB	
		(mg/kg)					percentage (%)	ROVA	percentage (%)	ROVA	percentage (%)	ROVA	percentage (%)	ROVA
1	Methyl acetate	1.5	C79209	$C_3H_6O_2$	272.703	1.19689	0.97 ± 0.06^{a}	3.07	0.36 ± 0.01^{b}	1.08	0.38 ± 0.01^{b}	1.16	1.02 ± 0.03^{a}	2.26
2	Ethyl acetate	32.55	C141786	$C_4H_8O_2$	301.175	1.33757	10.43 ± 0.22^{a}	1.52	16.72 ± 0.06^{a}	2.31	16.76 ± 0.2^{b}	2.36	6.93 ± 0.17^{c}	0.71
3	Ethyl butanoate	0.08	C105544	$C_6H_{12}O_2$	344.521	1.45854	1.69 ± 0.04^{a}	100.00	0.45 ± 0.01^{b}	25.34	0.46 ± 0.02^{b}	26.39	1.71 ± 0.04^{a}	71.02
4	Ethyl hexanoate	0.21	C123660	$C_8H_{16}O_2$	361.998	1.16871	0.49 ± 0.05^{b}	11.14	0.4 ± 0.02^{b}	8.58	0.39 ± 0.04^{b}	8.52	6.32 ± 0.28^{a}	100.00
5	Ethyl isobutyrate	0.057	C97621	$C_6H_{12}O_2$	308.865	1.25144	0.61 ± 0.07^{b}	50.67	0.25 ± 0.01^{c}	19.76	0.26 ± 0.02^{c}	20.94	0.88 ± 0.02^{a}	51.30
6	Ethyl lactate	128	C97643	$C_5H_{10}O_3$	883.494	1.54335	0.52 ± 0.01^{b}	0.02	1.49 ± 0.3^{a}	0.05	1.46 ± 0.33^{a}	0.05	0.31 ± 0.05^{b}	0.01
7	Ethyl propanoate	19.19	C105373	$C_5H_{10}O_2$	344.521	1.45854	0.63 ± 0.14^{a}	0.16	0.46 ± 0.01^{b}	0.11	0.48 ± 0.04^{b}	0.11	0.82 ± 0.03^{a}	0.14
8	1-Propanol	53.95	C71238	C_3H_8O	417.144	1.24637	5.31 ± 0.77^{b}	0.47	5.68 ± 0.07^{a}	0.47	5.61 ± 0.08^{a}	0.48	4.49 ± 0.03^{c}	0.28
9	2-Butanol	5.1	C78922	$C_4H_{10}O$	399.672	1.32404	0.49 ± 0.01^{b}	0.45	0.33 ± 0.01^{c}	0.29	0.34 ± 0.02^{c}	0.31	8.02 ± 0.06^{a}	5.23
10	Methanol	30	C67561	CH_4O	282.227	0.98091	1.63 ± 0.59^{a}	0.26	0.72 ± 0.19^{a}	0.11	0.88 ± 0.01^{a}	0.13	1.12 ± 0.06^{a}	0.12
11	2-Methyl-1-propanol	8	C78831	$C_4H_{10}O$	485.01	1.36619	8.3 ± 0.08^{c}	4.92	9.17 ± 0.1^{b}	5.16	9.13 ± 0.09^{b}	5.24	11.68 ± 0.07^{a}	4.85
12	3-Methyl-1-butanol (D)	0.7	C123513	$C_5H_{12}O$	674.134	1.49185	13.23 ± 0.85^{b}	89.59	15.54 ± 0.19^{a}	100.00	15.25 ± 0.27^{a}	100.00	15.35 ± 0.4^{a}	72.86
13	3-Methyl-1-butanol (M)	0.7	C123513	$C_5H_{12}O$	672.828	1.24185	1.99 ± 0.1^{b}	13.45	2.95 ± 0.15^{a}	18.98	3.13 ± 0.06^{a}	20.52	1.39 ± 0.05^{c}	6.60
14	Ethanol	2900	C64175	C_2H_6O	328.019	1.12411	28.6 ± 0.22^{b}	0.05	30.34 ± 0.01^{a}	0.05	30.28 ± 0.22^{a}	0.05	22.51 ± 0.26^{c}	0.03
15	Acetic acid (D)	120	C64197	$C_2H_4O_2$	1175.647	1.26573	17.79 ± 0.39^{a}	0.70	9.58 ± 0.61^{c}	0.36	9.73 ± 0.09^{c}	0.37	10.59 ± 0.39^{b}	0.29
16	Acetic acid(M)	120	C64197	$C_2H_4O_2$	1182.177	1.14915	0.84 ± 0.08^{a}	0.03	0.46 ± 0.07^{b}	0.02	0.41 ± 0.04^{b}	0.02	0.35 ± 0.01^{b}	0.01
17	Acrolein	0.21	C107028	C_3H_4O	270.798	1.06398	0.48 ± 0.19^{a}	10.86	0.34 ± 0.09^{a}	7.29	0.47 ± 0.02^{a}	10.27	0.34 ± 0.05^{a}	5.38
18	2-Methylpropanal (D)	0.1	C78842	C_4H_8O	308.469	1.06151	0.37 ± 0.1^{a}	17.36	0.31 ± 0.05^{a}	13.96	0.35 ± 0.00^{a}	16.07	0.23 ± 0.03^{a}	7.64
19	2-Methylpropanal (M)	0.1	C78842	C_4H_8O	302.922	1.02817	0.43 ± 0.19^{a}	20.26	0.17 ± 0.04^{a}	7.66	0.21 ± 0.00^{a}	9.64	0.13 ± 0.02^{a}	4.32
20	Propanal (D)	0.2	C123386	C_3H_6O	259.117	1.14999	0.86 ± 0.23^{a}	20.47	0.64 ± 0.11^{a}	14.41	0.56 ± 0.02^{a}	12.85	0.85 ± 0.05^{a}	14.12
21	Propanal (M)	0.2	C123386	C_3H_6O	260.193	1.04303	1.16 ± 0.39^{a}	27.49	1.72 ± 0.07^{a}	38.74	1.7 ± 0.03^{a}	39.02	1.05 ± 0.09^{a}	17.44
22	2-Butanone	3	C78933	C_4H_8O	308.865	1.25144	0.18 ± 0.01^{b}	0.28	0.15 ± 0.01^{b}	0.23	0.15 ± 0.00^{b}	0.23	1.36 ± 0.03^{a}	1.51
23	3-Hydroxy-2-butanone	0.75	C513860	$C_4H_8O_2$	783.84	1.33595	0.1 ± 0.00^{b}	0.61	0.21 ± 0.05^{a}	1.26	0.23 ± 0.04^{a}	1.41	0.13 ± 0.00^{a}	0.58
24	Acetone	100	C67641	C_3H_6O	268.799	1.11912	2.64 ± 0.06^{a}	0.13	1.4 ± 0.08^{c}	0.06	1.24 ± 0.02^{c}	0.06	2.21 ± 0.07^{b}	0.07
25	Dimethyl sulfide	1.1	C75183	C_2H_6S	282.227	0.98091	0.28 ± 0.05^{a}	1.20	0.16 ± 0.01^{a}	0.66	0.17 ± 0.03^{a}	0.71	0.23 ± 0.03^{a}	0.69

a–d different letters next to mean values indicates statistically significant difference ($p < 0.05$).

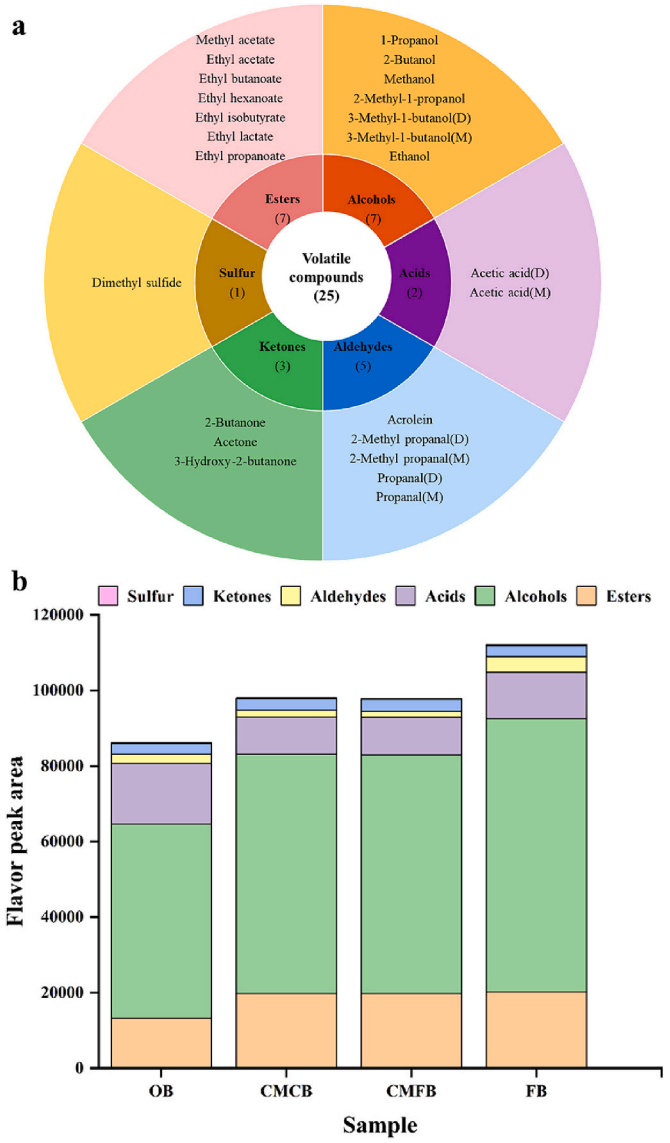

Fig. 5. Comparison of volatile compounds in different brandies(a) comparison of type and number; (b) comparison of flavor peak area.

was that the concentration of Ethyl hexanoate increases during the aging process, and the Ethyl acetate evaporates.

Alcohols: Alcohols were important aromatic compounds in brandy, mainly produced during fermentation from amino acids (Fan & Qian, 2005). A total of 7 volatile alcohols were identified in brandy, including 1-propanol, 2-butanol, 2-methyl-1-propanol, 3-methyl-1-butanol (D), 3-methyl-1-butanol (M), ethanol, and methanol. In addition to Ethanol, which was the main component of brandy, the following are 2-methyl-1-propanol and 3-methyl-1-butanol. They were higher alcohols that produce fusel smell and were also considered to be the odor of some wines. Key odor activities in products such as whiskey (Jeleń, Majcher, & Szwengiel, 2019). There was no significant difference in the relative content of alcohols in CMCB, CMFB and FB, both above 64%, while the relative content in the OB is low. The reason was that higher levels of alcohols such as 2-Methyl-propanol, 3-Methylbutanol and 2-Butanol were detected in the head and tail fractions, which increased the content of alcohols in the recombined wine compared to the OB (Tian et al., 2022).

Acids: Volatile acids originated from the alcoholic fermentation process and were important flavor substances in brandy (Zhao et al., 2012). The identified acids overall had low concentration in brandy, but it was important for acids to balance the taste of brandy. Only acetic acid was detected in the brandy, and the relative content of acid in FB is lower than other brandy. Studies had shown that during fermentation and aging, some acids and esters were esterified to generate esters (Zhao, Xu, Li, Fan, & Jiang, 2009), thereby reducing the content of acids in the finished brandy.

Aldehydes and ketones: Aldehydes and ketones were mainly derived from raw materials and fermentation processes. The aldehydes isolated and identified in brandy were acrolein, 2-Methyl propionaldehyde(D), 2-Methyl propionaldehyde(M), Propionaldehyde (D) and Propionaldehyde (M). The number of ketones was relatively low compared to aldehydes, with only 3 ketones detected, including 2-Butanone, 3-Hydroxy-2-butanone, and Acetone. Compared with FB, the relative content in the other three brandies was lower. However, in FB, the content of ketones was higher than aldehydes.

Sulfur: Although the concentration of volatile sulfur-containing compounds was low, it played a very important role in the flavor profile of wine, which mainly came from the degradation of sulfur-containing amino acids during fermentation (Dziekonska-Kubczak et al., 2020). Dimethyl disulfur was the only sulfur-containing compound found in brandy samples, and the content of sulfur-containing compounds in recombined brandy was slightly lower than FB. Although the smell of sulfur-containing compounds was unpleasant, when they were diluted to ppb and ppm levels, their flavor changed greatly, showing the spicy and nutty aromas of onion and garlic, which had a great impact on the aroma of various foods and beverages (Mestres, Busto, & Guasch, 2000). Low-molecular-weight volatile sulfur compounds were the main cause of reducing flavor and deteriorating quality in wine (Wang, Jia, et al., 2023; Wang, Ma, et al., 2023). In order to remove the reducing flavor imparted by H_2S, mercaptans, and so forth, copper was often deliberately added to wine to repress reductive off-flavor (Zhang et al., 2021). Compared with the finished brandy, the Cu (II) in CMF had reduced the content of volatile sulfur compounds in brandy.

3.10. The key volatile compounds by ROAV of different brandy

Relative odor activity value (ROAV) was commonly used to evaluate the contribution of volatile compounds (Bi et al., 2021). For all compounds, ROAV≤100; the larger the ROAV value, the greater the contribution of the component to the overall flavor of the sample. Compounds with ROAV≥1 were identified as key flavor compounds of the analyzed samples, and compounds with 0.1 ≤ ROAV<1 were identified as important modulators of the overall flavor of the sample. Sensory researches of wine had demonstrated that if the concentration of volatiles is above its odor perception threshold (ROAV>1), the aroma compound contributes to specific characteristics of flavor (Li et al., 2022). The ROAV values of 25 volatile compounds were shown in Table 6. There were 14 key flavor compounds and there were 8, 7, 7 and 7 embellished flavor compounds in OB, CMCB, CMFB and FB, respectively. Moreover, the ROAV values of Methyl acetate, Ethyl butanoate, Ethyl hexanoate, Ethyl isobutyrate, 2-Methyl-1-propanol, 3-Methyl-1-butanol (D), 3-Methyl-1-butanol (M), Acrolein, 2-Methylpropanal (D), 2-Methylpropanal (M), Propanal (D) and Propanal (M) were >1 in four brandies. The ROAV values of Ethyl propanoate, 1-Propanol, Methanol, and Acetic acid (D) were between 0.1 and 1 in four brandies. Therefore, there was little difference in the contribution of the above compounds to the flavor. However, the ROAV values of Ethyl acetate and 3-Hydroxy-2-butanone in CMCB and CMFB were both >1 and higher than FB. Research shows that Ethyl acetate had the aroma of fresh fruits and floral aroma, the addition of CMF improves the flavor of the blended brandy (Xu et al., 2022). In addition, the ROAV values for 2-Butanol in FB and Dimethyl disulfide in OB were >1, and some higher alcohols including 2-Butanol will increase the bitterness of the wine, thereby affecting the taste of the wine (Fan, Tang, Xu, & Chen, 2020). That shows the addition of CMF can reduce the ROAV value of brandy 2-

Butanol and Dimethyl disulfide.

3.11. Identification and content analysis of volatile compounds of different brandy

In order to further compare the flavor materialization law and relative content differences of volatile substances in the four brandies, the Gallery fingerprint was drawn according to the change of signal ion peak, and the results are shown in Fig. 6(a). Throughout the fingerprint, the data were arranged according to four different brandies. The sample in the figure is ordinate, the volatile substance composition was abscissa, and the color shade reflects the difference in volatile content (Chen, Farag, et al., 2021; Chen, Li, et al., 2021). There was a significant difference in the content of the four brandy volatile substances. In the area marked by a red rectangle, the content of ethyl Acetate, Acrolein, Ethyl lactate and 3-Hydroxy-2-butanone in CMCB and CMFB were significantly higher than OB and FB; in the area marked with a yellow rectangle, it can be seen that there were many types of flavor substances in the four brandies, and there was no significant difference in the content of each volatile substance, mainly including Propionaldehyde (M), Propionaldehyde (D), 2-Methyl-1-propionaldehyde (M), 2-Methyl-1-propionaldehyde (D), Acetic acid (M), Acetic acid (D), Methyl-1-propanol, Ethanol, 3-Methyl-1-butanol (M), 3-Methyl-1-butanol (D) and 1-Propanol; in the area marked with a green rectangle, there were 7 volatile compounds such as Ethyl butyrate, Ethyl isobutyrate, Dimethyl disulfide, Methyl acetate, Ethyl propionate, Methanol and Acetone, among which the content of volatile substances in the FB was richer, followed by the OB, and the content in the two recombined brandy was the least; in the area marked with a purple rectangle, 2-Butanol, Ethyl caproate, 2-Butanone were unique flavor substances in FB, which were hardly detected in the other three brandies.

To facilitate a clearer comparison among brandies, hierarchical cluster analysis (HCA) was utilized to explore the relationship between flavor compounds and brandies. As shown in Fig. 6(b), the heat map

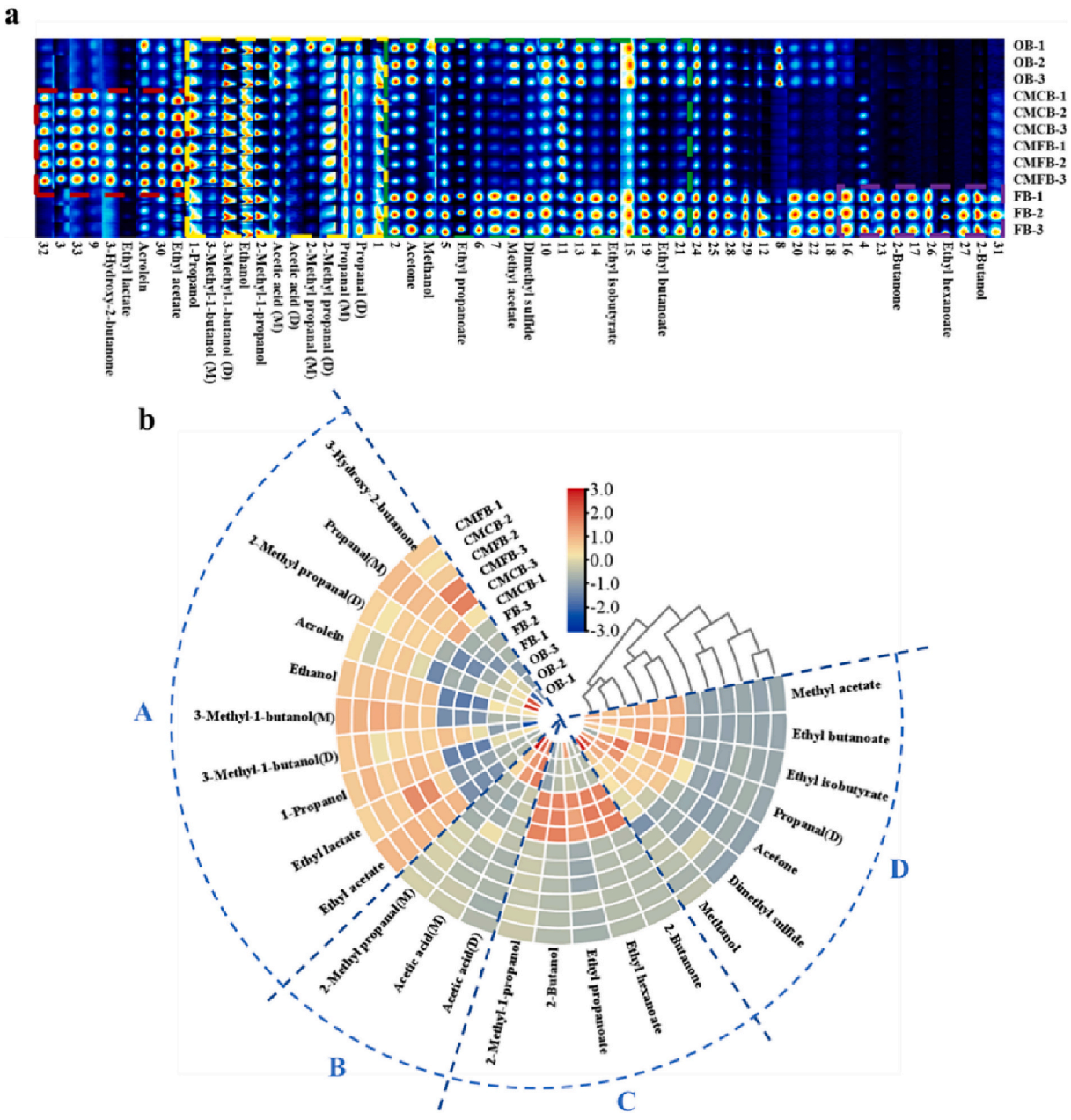

Fig. 6. Volatile compounds in four brandies(a) gallery plot fingerprint; (b) heat map clustering.

shows the average distribution of each compound in the samples with colored boxes, while the horizontal dendrogram indicated the clustering pattern among the samples (Ni, Yan, Tian, Zhan, & Zhang, 2022). The standardized color intensity scale ranged from the highest (dark red) to the lowest (dark blue), showing the relative contents of various volatile chemicals from high to low. The brandies were segregated into three clusters based on their flavor profiles. The first cluster was represented by OB, characterized by a higher proportion of aldehydes (Propanal, 2-Methyl propanal and Acrolein) and esters (Methyl acetate, Ethyl butanoate and Ethyl isobutyrate). The second cluster was exhibited by FB, which had a higher proportion of esters (Methyl acetate, Ethyl butanoate and Ethyl isobutyrate). The third cluster was described by CMCB and CMFB, with a higher proportion in alcohols (3-Methyl-1-butanol, Ethanol and 1-Propanol) (Jara-Palacios, 2019; Zhao et al., 2018). These results suggested that there were dramatic differences in flavor compounds between the four brandies. The HCA results provided insights into the differences in flavor profiles of the brandies, with potential implications for their production and marketing. Also, volatiles could be assigned to four groups based on the dendrogram. Group A comprised 10 compounds with higher content in CMFB and CMCB, and lower or almost no content in OB and FB. Group B contained 3 compounds that were at higher content in OB, including Acetic acid (D)、Acetic acid(M) and 2-Methyl propanal (M). Group C contained 5 compounds that were at higher content in FB, including 2-Methyl-1-propanol, Ethyl propanoate, 2-Butanol, Ethyl hexanoate and 2-Butanone. The remaining 7 compounds were classified as group D, which presented higher contents in FB and OB.

4. Conclusion

According to the data, it is found that the D401 resin is effective in removing Cu (II) from the distillation, achieving a maximum elimination rate of 97% for 62.25 mg/L of Cu (II), pH without adjusting, and 0.3 g of adsorbent at 25 °C. The results of three antioxidant assays demonstrates that all the samples exhibited excellent antioxidant capacity with the order of CMFB > CMCB > FB, which correlated with its compound content. GC-IMS analysis reveals the identification of 25 flavor substances in the brandy, including esters, alcohols, acids, aldehydes and ketones, with esters and alcohols being predominant. The alcohol content in the recombined brandy is slightly lower than the finished brandy, although no significant difference is observed in other compounds. By blending the treated distillation residue with Chinese wolfberry distillation pulp, the prepared brandy not only has the characteristics of commercial brandy, but also contains an increased content of bioactive substances, thus improving its antioxidant ability. The most crucial aspect is to simplify the production process of brandy. In conclusion, the distilling wastewater of Chinese wolfberry brandy could be effectively treated and re-utilized, resulting in the production of mixed brandy and maximizing the value of distilled residual in the processing industry.

CRediT authorship contribution statement

Yan Dang: Writing – original draft, Software, Methodology, Investigation, Data curation. **Qing-An Zhang:** Writing – review & editing, Supervision, Project administration, Funding acquisition, Conceptualization. **Zhi-Hui Zhao:** Validation, Software, Formal analysis.

Declaration of competing interest

The authors declare that they have no known competing financial interests or personal relationships that could have appeared to influence the work reported in this paper.

Data availability

Data will be made available on request.

Acknowledgements

This study was funded by National Natural Science Foundation of China [No. 31972206], Key Research Development Program of Shaanxi Province, China [No. 2021NY-163], Major Special Project of Erdos Science and Technology, Inner Mongolia, China [No. 2022EEDSKJZDZX022], and the Fundamental Research Funds for the Central Universities of China [No. GK202102009].

Appendix A. Supplementary data

Supplementary data to this article can be found online at https://doi.org/10.1016/j.fochx.2024.101380.

References

An, Y., Zheng, H., Sun, Q., Zheng, X., Liu, W., Tang, X., & Xiong, Z. (2020). Two-step synthesis of a single-layer grafting self-floating adsorbent for anionic dyes adsorption, surface separation and concentration. *Journal of Hazardous Materials, 384*, Article 121262. https://doi.org/10.1016/j.jhazmat.2019.121262

Bansal, M., Singh, D., & Garg, V. K. (2009). A comparative study for the removal of hexavalent chromium from aqueous solution by agriculture wastes' carbons. *Journal of Hazardous Materials, 171*, 83–92. https://doi.org/10.1016/j.jhazmat.2009.05.124

Bao, J., Wang, X., Gu, J., Dai, X., Zhang, K., Wang, Q., Ma, J., & Peng, H. (2020). Effects of macroporous adsorption resin on antibiotic resistance genes and the bacterial community during composting. *Bioresource Technology, 295*, Article 121997. https://doi.org/10.1016/j.biortech.2019.121997

Benitez, P., Castro, R., & Barroso, C. G. (2001). Removal of iron, copper and manganese from white wines through ion exchange techniques:Effects on their organoleptic characteristics and susceptibility to browning. *Analytica Chimica Acta, 458*, 192–202. https://doi.org/10.1016/S0003-2670(01)01499-4

Bhattacharjee, C., Saxena, V. K., & Dutta, S. (2017a). Fruit juice processing using membrane technology: A review. *Innovative Food Science and Emerging Technologies, 43*, 136–153. https://doi.org/10.1016/j.ifset.2017.08.002

Bhattacharjee, C., Saxena, V. K., & Dutta, S. (2017b). Watermelon juice concentration using ultrafiltration: Analysis of sugar and ascorbic acid. *Food Science and Technology International, 23*, 637–645. https://doi.org/10.1177/1082013217714672

Bi, J., Lin, Z., Li, Y., Chen, F., Liu, S., & Li, C. (2021). Effects of different cooking methods on volatile flavor compounds of chicken breast. *Journal of Food Biochemistry, 45*, Article e13770. https://doi.org/10.1111/jfbc.13770

Bonic, M., Tesevic, V., Nikicevic, N., Cvejic, J., Milosavljevic, S., Vajs, V., Mandic, B., Urosevic, I., Velickovic, M., & Jovanic, S. (2013). The contents of heavy metals in Serbian old plum brandies. *Journal of the Serbian Chemical Society, 78*(93), 3–945. https://doi.org/10.2298/jsc121106016b

Cassano, A., Conidi, C., & Tasselli, F. (2014). Clarification of pomegranate juice (*Punica Granatum* L.) by hollow fibre membranes: Analyses of membrane fouling and performance. *Journal of Chemical Technology & Biotechnology, 90*, 859–866. https://doi.org/10.1002/jctb.4381

Chen, F., Huang, G., Yang, Z., & Hou, Y. (2019). Antioxidant activity of Momordica charantia polysaccharide and its derivatives. *International Journal of Biological Macromolecules, 138*, 673–680. https://doi.org/10.1016/j.ijbiomac.2019.07.129

Chen, K., Li, S., Yang, H., Zou, J., Yang, L., Li, J., & Ma, L. (2021). Feasibility of using gas chromatography-ion mobility spectrometry to identify characteristic volatile compounds related to brandy aging. *Journal of Food Composition and Analysis, 98*, Article 103812. https://doi.org/10.1016/j.jfca.2021.103812

Chen, W., Zhu, J., Niu, H., Song, Y., Zhang, W., Chen, H., & Chen, W. (2018). Composition and characteristics of Yam juice fermented by lactobacillus plantarum and streptococcus thermophilus. *International Journal of Food Science & Technology, 14*, Article 20180123. https://doi.org/10.1515/ijfe-2018-0123

Chen, Z. J., Farag, M. A., Zhong, Z. F., Zhang, C., Yang, Y., Wang, S. P., & Wang, Y. T. (2021). Multifaceted role of phyto-derived polyphenols in nanodrug delivery systems. *Advanced Drug Delivery Reviews, 176*, Article 113870. https://doi.org/10.1016/j.addr.2021.113870

Chu, S. Y., Feng, X. F., Liu, C. C., Wu, H. R., & Liu, X. B. (2022). Advances in chelating resins for adsorption of heavy metal ions. *Industrial & Engineering Chemistry Research, 61*, 11309–11328. https://doi.org/10.1021/acs.iecr.2c01353

Dang, Y., Zhao, Z. H., Dong, J. F., Dang, W. H., & Zhang, Q.-A. (2022). Study on the nutritional composition and volatile substances of Chinese Wolfberry brandy distillation residue. *Journal of Hainan Normal University, 35*, 152–159.

Dziekonska-Kubczak, U., Pielech-Przybylska, K., Patelski, P., & Balcerek, M. (2020). Development of the method for determination of volatile sulfur compounds (VSCs) in fruit brandy with the use of HS-SPME/GC-MS. *Molecules, 25*, 1232–1246. https://doi.org/10.3390/molecules25051232

El-Ashtoukhy, E. S. Z., Amin, N. K., & Abdelwahab, O. (2008). Removal of lead (II) and copper (II) from aqueous solution using pomegranate peel as a new adsorbent. *Desalination, 223*, 162–173. https://doi.org/10.1016/j.desal.2007.01. 206

Fan, S., Tang, K., Xu, Y., & Chen, S. (2020). Characterization of the potent odorants in Tibetan Qingke Jiu by sensory analysis, aroma extract dilution analysis, quantitative analysis and odor activity values. *Food Research International, 137*, Article 109349. https://doi.org/10.1016/j.foodres.2020.109349

Fan, W., & Qian, M. C. (2005). Headspace solid phase microextraction and Gas Chromatography−Olfactometry dilution analysis of young and aged Chinese "Yanghe Daqu" liquors. *Journal of Agricultural and Food Chemistry, 53*, 7931–7938. https://doi.org/10.1021/jf051011k

Fan, X. H., Zhang, Q.-A., Yan, Y. Y., & Tian, C. R. (2016). Physicochemical properties and in-vitro antioxidant capacity of semen astragali complanati wine. *CyTA Journal of Food, 15*, 81–90. https://doi.org/10.1080/19476337.2016.1215350

Guo, X., Schwab, W., Ho, C. T., Song, C., & Wan, X. (2022). Characterization of the aroma profiles of oolong tea made from three tea cultivars by both GC-MS and GC-IMS. *Food Chemistry, 376*, Article 131933. https://doi.org/10.1016/j.foodchem.2021.131933

He, X., Fang, Z., Jia, J., Ma, L., Li, Y., Chai, Z., & Chen, X. (2014). Study on the treatment of wastewater containing Cu(II) by D851 ion exchange resin. *Desalination and Water Treatment, 57*, 3597–3605. https://doi.org/10.1080/19443994. 2014.986528

Hifney, A. F., Fawzy, M. A., Abdel-Gawad, K. M., & Gomaa, M. (2016). Industrial optimization of fucoidan extraction from Sargassum sp. and its potential antioxidant and emulsifying activities. *Food Hydrocolloids, 54*, 77–88. https://doi.org/10.1016/j.foodhyd.2015.09.022

Hoang, V. A., Nishihama, S., & Yoshizuka, K. (2021). Selective adsorption of lead(II) from aqueous solution. *Environmental Technology, 43*, 2124–2134. https://doi.org/10.1080/09593330.2020.1866088

Jara-Palacios, M. J. (2019). Wine lees as a source of antioxidant compounds. *Antioxidants, 8*, 45. https://doi.org/10.3390/antiox8020045

Jeleń, H. H., Majcher, M., & Szwengiel, A. (2019). Key odorants in peated malt whisky and its differentiation from other whisky types using profiling of flavor and volatile compounds. *LWT - Food Science and Technology, 107*, 56–63. https://doi.org/10.1016/j.lwt.2019.02.070

Katiyar, R., Patel, A. K., Nguyen, T. B., Singhania, R. R., Chen, C. W., & Dong, C. D. (2021). Adsorption of copper (II) in aqueous solution using biochars derived from ascophyllum nodosum seaweed. *Bioresource Technology, 328*, Article 124829. https://doi.org/10.1016/j.biortech.2021.124829

Korotkov, E., Stanislavskaya, E., & Melnikova, E. (2015). Preparation and use of whey protein microparticulate in synbiotic drink technology. *Foods Raw Mater, 3*, 96–104. https://doi.org/10.12737/13125

Kwaw, E., Ma, Y., Tchabo, W., Apaliya, M. T., Wu, M., Sackey, A. S., … Tahir, H. E. (2018). Effect of lactobacillus strains on phenolic profile, color attributes and antioxidant activities of lactic-acid-fermented mulberry juice. *Food Chemistry, 250*, 148–154. https://doi.org/10.1016/j.foodchem.2018.01.009

Lee, Y. M., Yoon, Y., Yoon, H., Park, H. M., Song, S., & Yeum, K. J. (2017). Dietary anthocyanins against obesity and inflammation. *Nutrients, 9*(10), 1089–1104. https://doi.org/10.3390/nu9101089

Li, S., Bi, P., Sun, N., Gao, Z., Chen, X., & Guo, J. (2022). Characterization of different non-Saccharomyces yeasts via mono-fermentation to produce polyphenol-enriched and fragrant kiwi wine. *Food Microbiology, 103*, Article 103867. https://doi.org/10.1016/j.fm.2021.103867

Li, S., Yang, H., Tian, H., Zou, J., & Li, J. (2020). Correlation analysis of the age of brandy and volatiles in brandy by gas chromatography-mass spectrometry and gas chromatography-ion mobility spectrometry. *Microchemical Journal, 157*, Article 104948. https://doi.org/10.1016/j.microc.2020.104948

Li, Z., Ren, Z., Zhao, L., Chen, L., Yu, Y., Wang, D., Mao, X., Cao, G., Zhao, Z., & Yang, H. (2023). Unique roles in health promotion of dietary flavonoids through gut microbiota regulation: Current understanding and future perspectives. *Food Chemistry, 399*, Article 133959. https://doi.org/10.1016/j.foodchem.2022.133959

Liang, F. B., Song, Y. L., Huang, C. P., Li, Y. X., & Chen, B. H. (2013). Synthesis of novel lignin-based ion-exchange resin and its utilization in heavy metals removal. *Industrial & Engineering Chemistry Research, 52*, 1267–1274. https://doi.org/10.1021/ie301863e

Lorenzo, C. D., Colombo, F., Biella, S., Stockley, C., & Restani, P. (2021). Polyphenols and human health: The role of bioavailability. *Nutrients, 13*, 273–303. https://doi.org/10.3390/nu13010273

Luo, Z., Guo, Z., Xiao, T., Liu, H., Su, G., & Zhao, Y. (2019). Enrichment of total flavones and licochalcone A from licorice residues and its hypoglycemic activity. *Journal of Chromatography B, 1114*, 134–145. doi: 10.1016/ j.jchromb.2019.01.026.

Mao, X. J., Xiao, W. M., Wan, Y. Q., Li, Z. M., Luo, D. M., & Yang, H. S. (2021). Dispersive solid-phase extraction using microporous metal-organic framework UiO-66: Improving the matrix compounds removal for assaying pesticide residues in organic and conventional vegetables. *Food Chemistry, 345*, Article 128807. https://doi.org/10.1016/j.foodchem.2020.128807

Matijasevic, S., Popovic-Djordjevic, J., Ristic, R., Cirkovic, D., Cirkovic, B., & Popovic, T. (2019). Volatile aroma compounds of brandy "Lozovaca" produced from Muscat table grapevine cultivars (*Vitis vinifera* L.). *Molecules, 24*, 2485–2500. https://doi.org/10.3390/molecules24132485

Mestres, M., Busto, O., & Guasch, J. (2000). Analysis of organic sulfur compounds in wine aroma. Journal of Chromatography A, 881, 569–581. doi: 10. 1016/ S0021–9673(00)00220-X.

Murota, K., Nakamura, Y., & Uehara, M. (2018). Flavonoid metabolism: The interaction of metabolites and gut microbiota. *Bioscience, Biotechnology, and Biochemistry, 82*, 600–610. https://doi.org/10.1080/09168451.2018.1444467

Neves, E. A., Oliveira, A., Fernandes, A. P., & Nóbrega, J. A. (2007). Simple and efficient elimination of copper(II) in sugar-cane spirits. *Food Chemistry, 101*, 33–36. https://doi.org/10.1016/j.foodchem.2005.12.050

Ni, R., Yan, H., Tian, H., Zhan, P., & Zhang, Y. (2022). Characterization of key odorants in fried red and green huajiao (Zanthoxylum bungeanum maxim. and Zanthoxylum schinifolium sieb. et Zucc.) oils. *Food Chemistry, 377*, Article 131984. https://doi.org/10.1016/j.foodchem.2021.131984

Niu, M., Huang, J., Jin, Y., Wu, C., & Zhou, R. (2017). Volatiles and antioxidant activity of fermented Goji (LyciumChinese) wine: Effect of different oak matrix (barrel, shavings and chips). *International Journal of Food Properties, 20*, 1–13. https://doi.org/10.1080/10942912.2017.1362649

Palacios, V. M., Caro, I., & Perez, L. (2000). Application of ion exchange techniques to industrial process of metal ions removal from wine. *Adsorption, 7*, 131–138. https://doi.org/10.1023/A:1011600207978

Raičević, D., Popović, T., Jančić, D., Šuković, D., & Pajović-Šćepanović, R. (2022). The impact of type of brandy on the volatile aroma compounds and sensory properties of grape brandy in Montenegro. *Molecules, 27*, 2974–2988. https://doi.org/10.3390/molecules27092974

Ren, J., Wang, S., Ning, Y., Wang, M., Wang, L., Zhang, B., & Zhu, B. (2018). The impact of over-maturation on the sensory and nutritional quality of Gouqi (Chinese wolfberry) wine. *Journal of the Institute of Brewing, 124*, 57–67. https://doi.org/10.1002/jib.469

Rodriguez-Mateos, A., Vauzour, D., Krueger, C. G., Shanmuganayagam, D., Reed, J., Calani, L., … Crozier, A. (2014). Bioavailability, bioactivity and impact on health of dietary flavonoids and related compounds: An update. *Archives of Toxicology, 88*, 1803–1853. https://doi.org/10.1007/s00 204-014-1330-7

Salian, R., Wani, S., Reddy, R., & Patil, M. (2018). Effect of brewery wastewater obtained from different phases of treatment plant on seed germination of chickpea (*Cicer arietinum*), maize (*Zea mays*), and pigeon pea (*Cajanus cajan*). *Environmental Science and Pollution Research, 25*, 9145–9154. https://doi.org/10.1007/s11356-018-1218-9

Schimek, D., Francesconi, K. A., Mautner, A., Libiseller, G., Raml, R., & Magnes, C. (2016). A matrix removal in state of the art sample preparation methods for serum by charged aerosol detection and metabolomics-based LC-MS. *Analytica Chimica Acta, 915*, 56–63. https://doi.org/10.1016/j.aca.2016.02.031

Song, Y., Ding, Z., Peng, Y., Wang, J., Zhang, T., Yu, Y., & Wang, Y. (2022). Acrylamide formation and aroma evaluation of fried pepper sauce under different exogenous Maillard reaction conditions. *Food Chemistry: X, 15*, 100413. doi: 10. 1016/j.fochx.2022.100413.

Szymczycha-Madeja, A., Welna, M., Jamroz, P., Lesniewicz, A., & Pohl, P. (2015). Advances in assessing the elemental composition of distilled spirits using atomic spectrometry. *TrAC Trends in Analytical Chemistry, 64*, 127–135. https://doi.org/10.1016/j.trac.2014.09.004

Tian, T. T., Ruan, S. L., Zhao, Y. P., Li, J. M., Yang, C., & Cao, H. (2022). Multi-objective evaluation of freshly distilled brandy: Characterisation and distribution patterns of key odour-active compounds. *Food Chemistry: X, 14*, Article 100276. https://doi.org/10.1016/j.fochx.2022.100276

Vyviurska, O., Matura, F., Furdíková, K., & Špánik, I. (2017). Volatile fingerprinting of the plum brandies produced from different fruit varieties. *Journal of Food Science and Technology, 54*, 4284–4301. https://doi.org/10.1007/s13197-017-2900-5

Wang, J., Ma, T., Wei, M., Lan, T., Bao, S., Zhao, Q., … Sun, X. (2023). Copper in grape and wine industry: Source, presence, impacts on production and human health, and removal methods. *Comprehensive Reviews in Food Science and Food Safety, 22*, 1794–1816. https://doi.org/10.1111/1541-4337. 13130

Wang, Q., Jia, X., Jin, M., Guo, R., Niu, B., Yan, H., & Wang, H. (2023). A magnetically recyclable carboxyl-functionalized chitosan composite for efficiently removing methyl orange from wastewater: Isotherm, kinetics, thermodynamic, and adsorption mechanism. *International Journal of Biological Macromolecules, 253*, Article 126631. https://doi.org/10.1016/j.ijbiomac.2023.126631

Wang, S., Chen, H., & Sun, B. (2020). Recent progress in food flavor analysis using gas chromatography-ion mobility spectrometry (GC-IMS). *Food Chemistry, 315*, Article 126158. https://doi.org/10.1016/j.foodchem.2019.126158

Xia, Y. N., Suo, R., Wang, H., Cerbin, S., & Wang, J. (2017). Analysis on flavor compounds of Jujube brandy from different fermentation heights by HS-SPME-GC/MS, E-nose and E-tongue. *Journal of Food Science and Technology, 12*, 332–344. https://doi.org/10.3923/ajft.2017.332.344

Xu, Y., Zhao, J., Liu, X., Zhang, C., Zhao, Z., Li, X., & Sun, B. (2022). Flavor mystery of Chinese traditional fermented baijiu: The great contribution of ester compounds. *Food Chemistry, 369*, Article 130920. https://doi.org/10.1016/j.foodchem.2021.130920

Yang, H., Su, W., Wang, L. H., Wang, C., & Wang, C. Y. (2021). Molecular structures of nonvolatile components in the Haihong fruit wine and their free radical scavenging effect. *Food Chemistry, 353*, Article 129298. https://doi.org/10.1016/j.foodchem.2021.129298

Zhang, L. L., Guan, Q. H., Jiang, J. C., & Khan, M. S. (2023). Tannin complexation with metal ions and its implication on human health, environment and industry: An overview. *International Journal of Biological Macromolecules, 253*, Article 127485. https://doi.org/10.1016/j.ijbiomac.2023.127485

Zhang, Q.-A., Fan, X. H., Zhao, W. Q., Wang, X. Y., & Liu, H. Z. (2013). Evolution of some physicochemical properties in Cornus officinalis wine during fermentation and storage. *European Food Research and Technology, 237*, 711–719. doi: 1007/s00217-013-2045-3.

Zhang, Q.-A., Zhang, X. L., Yan, Y. Y., & Fan, X. H. (2017). Antioxidant evaluation and composition analysis of extracts from Fuzhuan brick tea and its comparison with two instant tea products. *Journal of AOAC International, 100*, 653–660. https://doi.org/10.5740/jaoacint.16-0403

Zhang, X., Kontoudakis, N., Wilkes, E., Scrimgeour, N., Hirlam, K., & Clark, A. C. (2021). The removal of cu from wine by copolymer PVI/PVP: Impact on cu fractions and binding agents. *Food Chemistry, 357*, 129764. doi: 10. 1016/j.foodchem.2021.129764.

Zhao, L., Ren, J., Wang, L., Li, J., Wang, M., Wang, L., … Zhang, B. (2019). Evolution of sensory attributes and physicochemical indexes of Gouqi fermented wine under different aging treatments and their correlations. *Journal of Food Processing and Preservation, 43*, Article e13873. https://doi.org/10.1111/jfpp.13873

Zhao, Y., Xu, Y., Li, J., Fan, W., & Jiang, W. (2009). Profile of volatile compounds in 11 brandies by headspace solid-phase microextraction followed by gas chromatography-mass spectrometry. *Journal of Food Science, 74*, 90–99. https://doi.org/10.1111/j.1750-3841.2008.01029.x

Zhao, Y. P., Li, J. M., Zhang, B. C., Yu, Y., Shen, C. H., & Song, P. (2012). A comparison of the influence of eight commercial yeast strains on the chemical and sensory profiles of freshly distilled Chinese brandy. *The Journal of the Institute of Brewing, 118*, 315–324. https://doi.org/10.1002/jib.44

Zhao, Y. P., Zheng, X. P., Song, P., Sun, Z. L., & Tian, T. T. (2018). Characterization of volatiles in the six most well-known distilled spirits. *Journal of the American Chemical Society, 71*, 161–169. https://doi.org/10.1094/asbcj-2013-0625-01

Zhong, W., Li, X., Yang, H., & Li, E. (2018). A novel, effective, and feasible method for deacidifying kiwifruit wine by weakly basic ion exchange resins. *Journal of Food Process Engineering, 42*, Article e12969. https://doi.org/10.1111/jfpe.12969